



Flood Risk Zone Identification Using Multi-criteria Decision Approach

4

Raja Majumder and Gouri Sankar Bhunia

Abstract

Flooding phenomenon is deliberated as the world's vilest comprehensive risk in terms of scale, existence, geographical extent, forfeiture of life and goods along with dislodgment of people and demographic events. A flood risk map of the Bongaon sub-division was generated using multi-criteria decision approach (MCDA) through geographical dataset, viz. rainfall, elevation, slope, soil, geomorphology, distance of river to the main channel, vegetation vigor, fractional impervious surface, road density, land use/land cover. Fifty-five validation points are used to evaluate the flood hazard risk map. The validation result proposes that MCDA and geospatial technology are very influential approaches in flood risk analysis and mapping. The derived flood risk map was reclassified into five categories through manual classification methods in ArcGIS software, such as very low risk, low risk, medium risk, high risk, and very high risk. The flood risk map portrays that probably 74.70 km² (8.96%) of the area comes under very high flood risk areas. The medium flood risk areas are calculated as

242.02 km² (29.02%), distributed in the central north, north-west and south-west part of the study site. The overall user accuracy and producer accuracy of the flood risk map was calculated as 69% and 72%, respectively. Choosing suitable factors may be useful to planners and developers for future development and land use planning.

Keywords

Flood hazard · Multi-criteria decision approach · GIS · Flood control

4.1 Introduction

Flood hydrology covenants with the functionality of time and space reliant developments of waters and are engrossed on hydraulic and engineering magnitudes of floods. Flood in association with climate change and meteorological variability in the recent past in India have already been analyzed and discussed by several researchers (Guhathakurta et al. 2011; Nandargiand and Dhar 2003). Moreover, there is a substantial chronological dissimilarity in the monsoon rainfall connected to climatic erraticism in India. To generate the flood hazard map, numerous issues are required for accurate mapping under circumstances of data and other constituents' inadequacies that epitomize the condition in most of

R. Majumder (✉) · G. S. Bhunia
Department of Geography, Seacom Skills
University, Kendradangal, Santiniketan, Birbhum,
West Bengal 731236, India

the countries. In general, computable data of the flood predisposing factors derived through a number of specialists accordingly, the format and spatial resolution of the data illustration differs between various sources. Earlier several research studies were conducted using remote sensing and GIS technique to generate the flood inundation areas (Haq et al. 2012; Patel and Srivastava 2013; Ouma and Tateishi 2014; Kazakis et al. 2015; Roy and Sarker 2016; Dhruvesh et al. 2016). For the past two to three decades, researchers were elaborating on evolving dissimilar approaches and facsimiles for flood risk mapping using Remote Sensing and Geographical Information System (Dandapat and Panda 2018). Fuzzy logic (Nugraha et al. 2018), logistic regression (Lim and Lee 2018), analytical hierarchy process (Matori et al. 2014), artificial neural networks (Elsafi 2014), frequency ratio (Cao et al. 2016), multi-criteria decision support system (Samanta et al. 2016) and weights-of-evidence (Rahmati et al. 2016) are limited eminent and satisfactory approaches in natural hazard modelling for investigating the multifaceted difficulties in different parts of the world.

Floods are perhaps the most frequent, pervasive calamitous and recurrent natural hazards in India. North 24 Parganas are one of the most flood-prone regions in West Bengal (India) due to heavy rainfall in monsoon season, highly silted Ichamati River system, inadequate capacity to carry the high flood discharge (http://www.wbiwd.gov.in/uploads/ANNUAL_FLOOD_REPORT-2016.pdf), improper drainage, land use/land cover characteristics, geomorphology, etc. (Majumder et al. 2017). The human interferences subsidizing to flood events are principally in the practice of repossession of wetlands and surface water bodies, modification in land use configuration, creation of impenetrable linkages of roads, formation of extensive built-up areas, deforestation etc. Ajin et al. (2011) conducted a study to generate the flood risk maps of the Vamanapuram River basin reliant upon multi-criteria assessment using geospatial technologies. Ismail and Saanyol (2013) have conducted a research for the flood vulnerability

mapping in the Kaduna River of Nigeria using a digital elevation model (DEM) and hydrological analysis. Getahun and Gebre (2015) carried out the study on flood hazard assessment and mapping of flood inundation area of the Awash River Basin in Ethiopia using GIS and HEC-GeoRAS/HEC-RAS Model.

The flood vulnerability mapping demarcates risk areas in the Gangetic plain by assimilating local acquaintance, hydrological, climatological, and geomorphological data using various methods. Consequently, hazards hypothetically detrimental physical extent, the phenomenon for the feature of life or injury, property impairment, ecological dilapidation, socio-economic commotion (Getahun and Gebre 2015). The creation of a very high spatial resolution GIS database is costly and time-consuming. Recently, several investigations have been done to evaluate flood hazards using geospatial technology (Mandal and Mandal 2015). Frequency ratio (Tehrany et al. 2015), analytical hierarchy process (Stefanidis and Stathis 2013), fuzzy logic (Pradhan 2011), logistic regression (Fustos et al. 2017), artificial neural networks (Abdellatif et al. 2015), and weights of evidence (Tehrany et al. 2017) and multi-criteria decision support systems are few well known and acceptable methods in flood hazard modelling for analysing complex problems different regions.

Correct and up-to-date floodplain maps can be the most cherished tackles for evading unadorned social and fiscal victims from floods. One of the flood risk management against flood impact at the regional scale is the identification of vulnerable areas to provide early warning, facilitate quick response and decrease the impact of possible flood events. The aims of the present research work are to find out the appropriate conditioning factor of flood susceptibility of the Bongaon Sadar sub-division and its applicability in various regions. Therefore, the flood risk map of Bongaon Sadar sub-division was generated through multi-criteria decision approach (MCDA) based on the integration of remotely sensed products and secondary datasets.

4.2 Study Area

Bangaon subdivision is part of the Ichamati–Raimangal Plain, located in the North of the North 24 Parganas (West Bengal, India). Figure 4.1 shows the location of the map of the Bongaon subdivision. The sub-division is divided into 3 blocks, namely Bagda, Bangaon and Gaighata. Bongaon subdivision is particularly susceptible to flooding because of its physiography and tropical monsoon climate characterized by drenching rainfall and unplanned management of floods (Ghosh and Mistri 2015). The sub-division is a part of the lower Gangetic delta and is also remarkable on the vast gradational surface (Saha 2015). Bhagirathi and Hooghly River flow over the western side of the sub-division (Mondal and Bandyopadhyay 2014). Ichamati River flows through the center. Surface expression of normal fault is running through the Burdwan–Debagram–Jalangi area (Sengupta 1966), flowing through the eastern part of the North 24 Parganas (north and south) districts eventually exits in the Raimangal River *vis-à-vis* the Bay of Bengal. The annual temperature of the study area ranges between 8 and 41°C in January and May, respectively. The highest relative humidity of the study area is recorded as 80% in July. The annual average rainfall of the study area is calculated as 1,579 mm. The major crop of the study area is recorded as rice, wheat, pulses and other oil seeds. As per the 2011 census, the total population of the study area was recorded as 1,063,028, with a population density of 838.17 km². Bangaon subdivision had a literacy rate of 80.57%.

The dwindling of this Ichamati River can be accredited to extreme sedimentation load, lessening headwater supply, tidal interference, growth of cultivated land and numerous instinctive interferences into the river regime like the creation of bridges, road on the riverbed by intruding its natural flow (Saha 2015). Around 50% of the total population in Bongaon and almost 75% of its properties are placed in flood susceptible extents (http://cgwb.gov.in/documents/Bhujal_News_24_1.pdf). Several

number of life-threatening flood measures befell during the past two decades and instigating substantial mutilation to life and stuff acme the inevitability for suitable flood administration trials in the sub-division.

4.3 Materials and Method

4.3.1 Collection of Secondary Data

Quantitative methods are employed for the exploration of geometric data to inaugurate spatial associations stuck between causative factors and floods. To classify a flood risk zone, a multi-parametric dataset encompassing satellite data, conformist maps containing Survey of India (SOI) topographical sheets has been employed for the generation of thematic maps, like drainage density, built-up areas, road density and surface waterbody, etc.

4.3.2 Analysis of Flood Frequency

The most important factor for determining the flood hazard is flood frequency. Available data of flood occurrences for the decade 1996–2016 was obtained from the sub-divisional office of Bongaon, North 24 Parganas in West Bengal (India). This information was used to generate the frequency of flood occurrence in the study area. The flooded areas for each year were integrated into a single layer of the GIS database and polygon shapefile were prepared for each year.

4.3.3 Satellite Data Acquisition and Preprocessing

Landsat8 Operational Land Imager (OLI) data of two different time periods (Month of October and February) were acquired from the United States of Geological Survey (USGS) Earth Explorer community. The satellite data was radiometrically and geometrically corrected using ERDAS

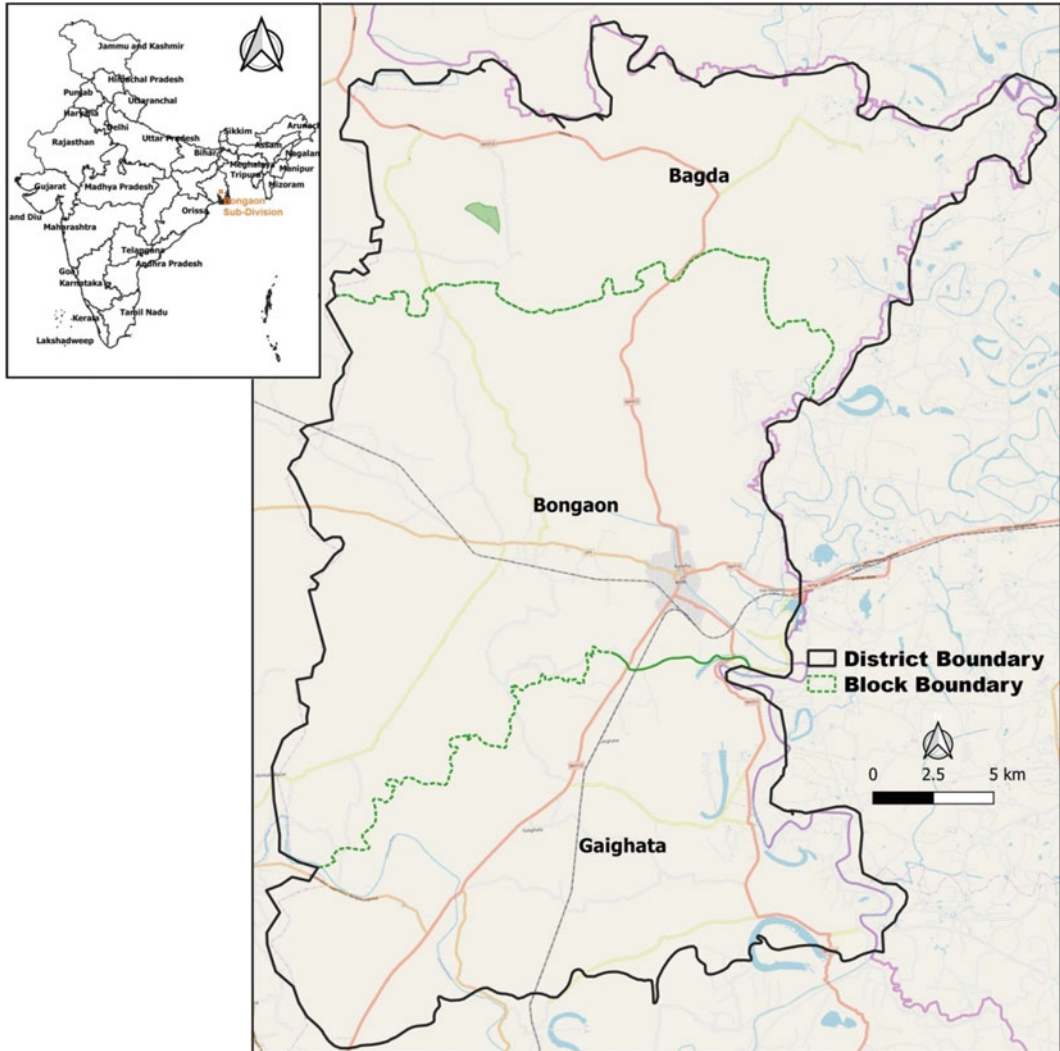


Fig. 4.1 Location map of Bongaon sub-division

Imagine software version 9.0. The Satellite data was geo-referenced in Universal Transverse Mercator (UTM) projection system and World Geodetic System (WGS) 84 datum. Advanced Space Thermal Emission Radiometer (ASTER) Global Digital Elevation Model (GDEM) data (2010) with a spatial resolution of 30 m was used for the topographical analysis, collected through the Earth Remote Sensing Data Analysis Center (ERSDAC) and the NASA Land Processes Distributed Active Archive Center (LP DAAC).

4.3.4 Rainfall Distribution

The rainfall data of the Bongaon sub-division and its surrounding station were collected from the IMD station. A total of five station data rainfall data of the past 10 years (2006–2016) were collected. The annual average rainfall data was calculated for each station. Finally, the rainfall distribution map of the study area was prepared using the radial basic function (RBF) method using ArcGIS spatial analyst tool.

4.3.5 Soil Characteristics

The soil map of the study area was acquired from the National Atlas Thematic Mapping Organization (NATMO), Kolkata, West Bengal, India, and finally validated with the published literature. The vector layer of the soil map of the Bongaon sub-division was prepared after geo-processing operation in ArcGIS software v9.3.

4.3.6 Distance of River to Main Channel and Drainage Density

Areas located close to the main river channel and flow accumulation path are more likely to get flooded (Islam and Sado 2000). Therefore, the polygon buffer of the main channel is created as 500 m, 1000 m, 1500 m, 2000 and more than 2500 m in ArcGIS software v9.3. Drainage network is first digitized from the SOI toposheet. After that, the drainage network has been validated with the Landsat8 Operational Land Imager (OLI) satellite data. The drainage density of the study area is calculated as follows:

$$D_d = \frac{\text{Total length of drainage channel in sq km}}{\text{Area (within 5sq km)}}$$

4.3.7 Surface Elevation and Slope:

Surface elevation is another natural factor that causes flood. In areas of higher elevation, the probability of flood occurrence is relatively lower than that of the lower elevation. In areas of lower elevation, the terrain is generally gentle, and the flow of water remains slow and holds the water for a long duration of time. The elevation map of the study area is derived through ASTER digital elevation model data. A slope map of the study areas is prepared from ASTER Digital Elevation Model (DEM) Data. The slope angle of each pixel is generated from ArcGIS software v9.3.

4.3.8 Geomorphology

By a combination of spectral band7 (SWIR 1.55–1.75 μm), band10 (TIR 10.40–12.50 μm) and band6 (NIR 0.77–0.90 μm) of Landsat8, image analysis was performed to identify the geomorphic characteristics like river/stream, abandoned channel, old and new alluvial plain, ox-bow lake, paleochannel, natural depressions, back swamps and meander scar. The geomorphological map was prepared with the evidence used by Chaturvedi and Mishra (2015) and Mukherjee (2006). After that, the selective field checks were performed to assess the validity of the pre-field image interpretation.

4.3.9 Analysing of Land Use/Land Cover and Vegetation Characteristics

The land use classes derived are often not satisfactory because of the limitation of spatial resolution in remote sensed imagery and the heterogeneity of urban landscapes. A range of impervious surfaces may be mixed with other land cover types such as forest, soils and pastures. Land use/land cover is an additional imperative persuading factor of flood hazard (Alexakis et al. 2014).

The vegetation characteristic of the study area was derived using a near-infrared and red band of OLI sensor data of Landsat8. The normalized difference vegetation index (NDVI) was calculated using channel 5 and channel4 of the landsat8 OLI sensor using the following equation:

$$NDVI = \frac{(\text{Near infrared}_{\text{Channel5}} - \text{Red}_{\text{Channel4}})}{\text{Near infrared}_{\text{channel5}} + \text{Red}_{\text{channel4}}}$$

4.3.10 Fractional Impervious Surface Area (FIS)

Impervious surface is demarcated as the surface avert water penetrates the soil and is mainly associated with conveyance and building

rooftops. FIS can be perceived and enumerated because of their massive topographical coverage and chronological occurrence of data collection, thus deciphered numerous ecological disputes such as land cover for hydrological and eco-friendly mockups. In this study, to calculate the FIS following equation has been followed:

$$FIS = 1 - FVC$$

where FVC refers to Fractional Impervious Surface Area.

FVC can be calculated using the following equation proposed by Calson and Ripley (1997):

$$FVC \approx (NDVI_s)^2$$

whereas, NDVI refers to normalized difference vegetation index. ND0VIs can be calculated using the following equation proposed by Basarudin and Adnan (2014).

$$NDVI_s = \frac{NDVI - NDVI_{low}}{NDVI_{high} - NDVI_{low}}$$

FVC ranges between 0 and 1.

4.3.11 Population Density

Population pressure is another important factor of the hazard map. A village-based vector layer is prepared from the entire sub-division and integrated with the GIS database based on 2011 census data. The population density of the study area is calculated as

$$\text{Population density} = \frac{\text{Total number of population in a village}}{\text{Area in km}^2}$$

4.3.12 Road Density

In this research, all the metalled, unmetalled and pucca village roads of the study area were digitized. All the roads were extracted primarily from the SOI topographical sheet and improved using Google Earth image in shapefile format. The

density is calculated as the length of the road per sq km. After that using the spatial analyst tool of ArcGIS software, the road density map was generated.

4.3.13 Multi-criteria Analysis

GIS-based multi-criteria decision analysis (MCDA) can be thought of as a process that combines and transforms spatial and aspatial data into a resultant decision. This practice is an arithmetical scheme reliant upon biophysical aspects, which are directly or circuitously associated with the event of floods. In this study, elevation, slope, drainage density, the distance of river to the main channel, vegetation vigour, fractional impervious surface, road density, land use/land cover were taken as the most important elements for appraising the flood hazard. Weights were consigned to the rasterized data layers and using map algebra in the spatial analyst tool to run a multi-criteria analysis. Subsequently, among the weighting measures, each aspect was segregated into five sub-factors, each of which was specified a ranking cost for the analogous sub-factor. For every aspect, the weighted influence ranking was attained by bourgeoning its burden by the ranking value for the analogous sub-types. The entire assessed threat, attained by tallying the weighted flood statuses of all the features were categorized into five classes—very low, low, moderate, high and very high. The overall methodology of the study area is illustrated in Fig. 4.2.

4.3.14 Verification and Observation

Finally, flood hazard risk maps were composed in the GIS platform and the maps were endorsed in the field to evaluate its exactitude. The procedure has been completed through a field visit to describe how meticulously the flood risk map settles with the concrete field condition. For the field justification, 55 GPS ground truth data of flood pretentious areas delineated organized with

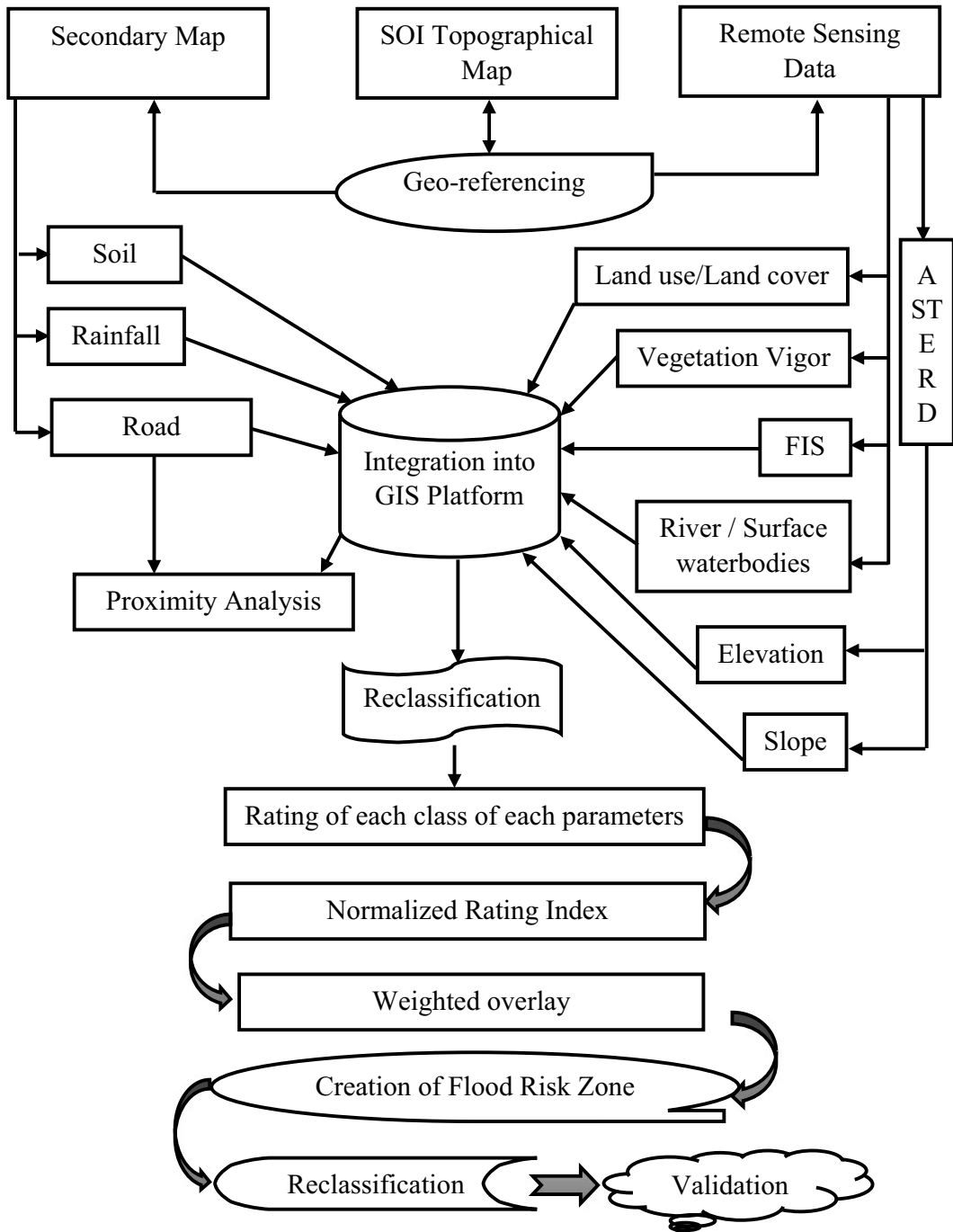


Fig. 4.2 Overall methodology of the research work

their corresponding LULC types were demarcated and a point shapefile has been generated. The LULC features that are set up within flood-

affected areas (e.g. built-up areas, cultivated land, agricultural fallow and landscapes located in a hazardous area) are confirmed at the field,

considered as a flood risk indicator. This point shapefile was superimposed with flood hazard and risk maps and then the flood hazard risk maps were verified with the actual field situations.

4.4 Results

The details of the flood pre-disposing factors were described in chapter VI, which are directly or circuitously associated with the happening of floods. All the features governing flood hazard layers were rehabilitated into raster format. Furthermore, these raster maps were reclassified. Weighted sum operation in spatial analysis extension of ArcGIS v9.3 was charted to assimilate all Normalized Rating Index (NRI) and Normalized Weight Index (NWI) and to produce a pixel by pixel (15 m spatial resolution) flood hazard and/or vulnerability database (Tables 4.1 and 4.2). The weights of the selective themes were consigned on a scale of 1 to 5 reliant upon

their impact on the flood menace. Apposite weights were allocated to the eleven aspects and their discrete aspects after understanding their importance in causing flood hazard occurrence in the sub-division. Among the elevation factors, LULC weighted the highest with 21%, followed by rainfall with 15%, slope with 13%, elevation with 8%, soil with 8%, road density with 8%, distance from the river by 7.5%, geomorphology by 7.5%, vegetation vigour by 7% and fractional impervious surface by 5%, respectively. The factors were weighted based on their virtual prominence to each other and to their estimated significance in initiating floods in the Bongaon sub-division. For every aspect, the subjective menace ranking was attained by multiplying its burden by the ranking worth for the conforming sub-factor.

Monthly rainfall data of five meteorological stations within the Bongaon sub-division for a period of (2005–2016) were obtained from the meteorological department. Monthly data were then converted to annual mean rainfall. The

Table 4.1 Rate, normalized rating index, weight index based on MCDA of flood hazard assessment of Bongaon sub-division

Parameters	Category/class	Rate	Normalized rating index (NRI) [Individual/total]	Weight (W)	Normalized weight index (NWI)
Rainfall (mm)	Less than 1450	5	0.33	15	1.5
	1451–1500	4	0.27		
	1501–1520	3	0.20		
	1521–1543	2	0.13		
	More than 1543	1	0.07		
Elevation (m)	<5.0 m	5	0.38	8	0.8
	5.1–7.5	4	0.31		
	7.6–10.0	3	0.23		
	>10.1	1	0.08		
Slope (degree)	Less than 1.0°	5	0.33	13	1.3
	1.1–1.5°	4	0.27		
	1.6–2.0°	3	0.20		
	2.1–4.0°	2	0.13		
	More than 4.1°	1	0.07		

(continued)

Table 4.1 (continued)

Parameters	Category/class	Rate	Normalized rating index (NRI) [Individual/total]	Weight (W)	Normalized weight index (NWI)
Land use/land cover	River/surface waterbodies	5	0.28	21	2.1
	Low laying area	4	0.22		
	Moist fallow	3	0.17		
	Built-up area	1	0.06		
	Agricultural fallow	2	0.11		
	Crop land	3	0.17		
Vegetation vigour (NDVI)	<0.0098	5	0.33	7	0.7
	0.0099–0.16	4	0.27		
	0.17–0.23	3	0.20		
	0.24–0.50	2	0.13		
	>0.50	1	0.07		
Fractional impervious surface	<20	1	0.10	5	0.5
	21–35	2	0.20		
	36–50	3	0.30		
	>51	4	0.40		

Table 4.2 Rate, normalized rating index, weight index based on MCDA of flood hazard assessment of Bongaon sub-division

Parameters	Category/class	Rate	Normalized rating index (NRI) [Individual/total]	Weight (W)	Normalized weight index (NWI)
Geomorphology	Abandoned channel	3	0.07	7.5	0.75
	Active river channel	5	0.12		
	Back swamp	3	0.07		
	Channel bar	5	0.12		
	Deep depression	4	0.09		
	Meander scar	5	0.12		
	Newer alluvial plain	4	0.09		
	Older alluvial plain	2	0.05		
	Older alluvial plain- type ii	1	0.02		
	Ox-bow lake	4	0.09		
	Paleochannel	4	0.09		
	Shallow depression	3	0.07		

(continued)

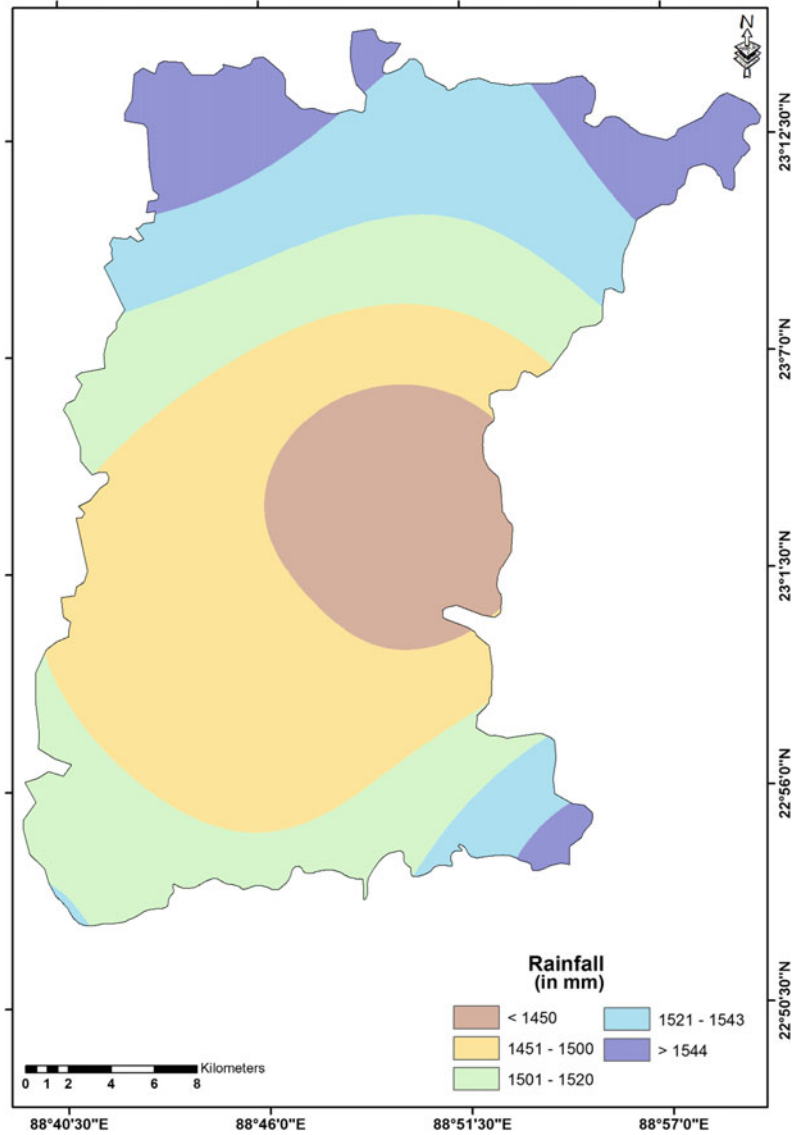
Table 4.2 (continued)

Parameters	Category/class	Rate	Normalized rating index (NRI) [Individual/total]	Weight (W)	Normalized weight index (NWI)
Soil Type	Very deep to deep, poorly drained, fine loamy to fine	5	0.25	8	0.8
	Very deep, fine loamy, poorly to imperfectly drained	4	0.2		
	Very deep, fine loamy, poorly to moderately well drained, fine loamy	2	0.1		
	Very deep, moderately well to poorly drained, coarse loamy to fine	2	0.1		
	Very deep, poorly drained, fine loamy	3	0.15		
	Very deep, poorly to moderately well drained, fine to coarse loamy	3	0.15		
	Very deep, poorly to well drained, fine to sandy	1	0.05		
Distance from the river (m)	Less than 500	5	0.33	7.5	0.75
	501–1000	4	0.27		
	1001–1500	3	0.20		
	1501–2000	2	0.13		
	More than 2001	1	0.07		
Road density (km ²)	<0.59	1	0.07	8	0.8
	0.60–0.76	2	0.13		
	0.77–0.92	3	0.20		
	0.93–1.1	4	0.27		
	>1.2	5	0.33		

average annual rainfall map was prepared through radial basis function and the rainfall map was divided into five categories (Fig. 4.3). In the classification process, the sub-division with higher rainfall (mm) is assigned 1 as it would be very extremely pretentious by a flood. The elevation map of the study area was prepared through ASTER satellite data and the Bongaon sub-division was categorized into 4 sub-categories of elevation zone (Fig. 4.4). Areas with the lowest elevation zone were considered as most vulnerable to flooding, thus ranked 1 which is less than 5.0 m. Following the flood hazard classes, there were the class high (5.1 m–7.5 m) ranked 2, class moderate (7.6 m–10.0 m)

ranked 3 and class low (>10.1 m) very low ranked 4. The slope layer of the Bongaon sub-division was prepared from the ASTER Digital Elevation Model (DEM) data and reclassified into five sub-categories in the order of flood hazard rating. The ASTER DEM was downloaded from USGS Earth Explorer Community (<https://earthexplorer.usgs.gov/>). The pixel resolution of ASTER DEM data is 30 m considered for this analysis. In the present research, less than 1° slope is considered as high risk for flood hazard (Fig. 4.5). LULC characteristics of the sub-division were reclassified into a common scale permissible of their rainwater intellection capabilities for the flood hazard examination into

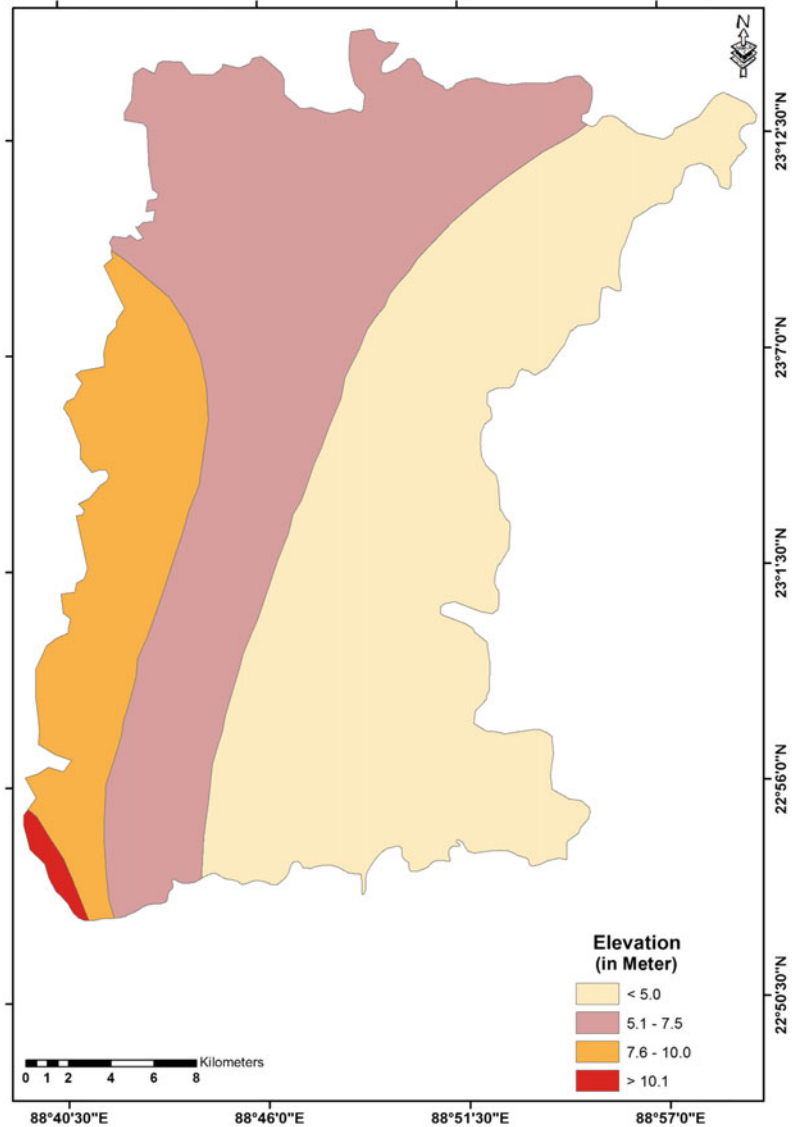
Fig. 4.3 Reclassified rainfall map of Bongaon sub-division



flood evaluation outcomes for land cover element map (Fig. 4.6) Based on the flood causing physiognomies of the LULC types, river and/or surface water bodies as a very high rating, low laying area was assigned high flooding, moist fallow and crop land were assigned as moderate class, agricultural fallow was demarcated as low rating and the built-up area was assigned as very low rating. Vegetation characteristics designate the presence of the landscapes and are commonly categorized by the amount and form of vegetation, which reflects its usage, milieu, agronomy

and cyclic phenology. The vegetation characteristics of the Bongaon sub-division have been classified into five sub-zones (Fig. 4.7). The low-density vegetation cover was assigned as a high rating for flood vulnerability and the high-density vegetation cover was demarcated as a low rating for flood hazard. The reclassified map of fractional impervious surface (FIS) of the Bongaon sub-division is illustrated in Fig. 4.8. The lower FIS value implies a higher permeability, whereas the higher FIS value indicated lesser permeability. The geomorphological characteristics of the

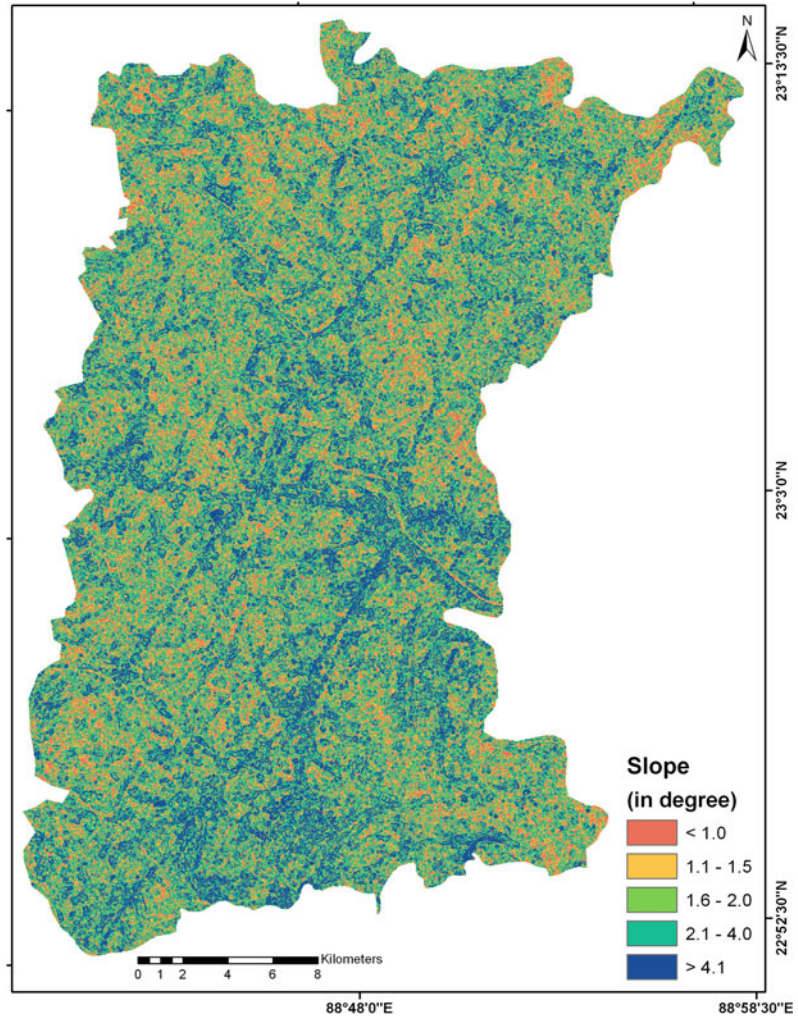
Fig. 4.4 Reclassified elevation map of Bongaon sub-division



sub-division play an important role in flood hazard susceptibility. In the Bongaon sub-division, new alluvial plain zones, channel bar and meander scar were providing a high rating for flood risk (Fig. 4.9). High to moderate flood vulnerability areas were demarcated as abandoned river channel, paleochannel, ox-bow lake, back swamp and deep depression due to the location adjacent to the very high susceptibility zone. Moreover, the low flood susceptibility zone was assigned as an older alluvial plain and shallow depression (Table 4.2). In this research,

very deep to deep, poorly drained, fine loamy to fine soil has been assigned higher weightage and the very deep, poorly to well drained, fine to sandy has been assigned the lower rating (Fig. 4.10). Moreover, very deep, poorly to well drained, fine to sandy soil was demarcated as a low rating of flood hazard. Finally, the soil map was transformed into raster format and reclassified based on their water infiltration capacity into flood rating results for the soil factor map (Table 4.2). Less than 500 m distance from the active river channel is considered as more prone

Fig. 4.5 Reclassified slope map of Bongaon sub-division (Slope map was generated from ASTER DEM Data; Spatial resolution—30 m)



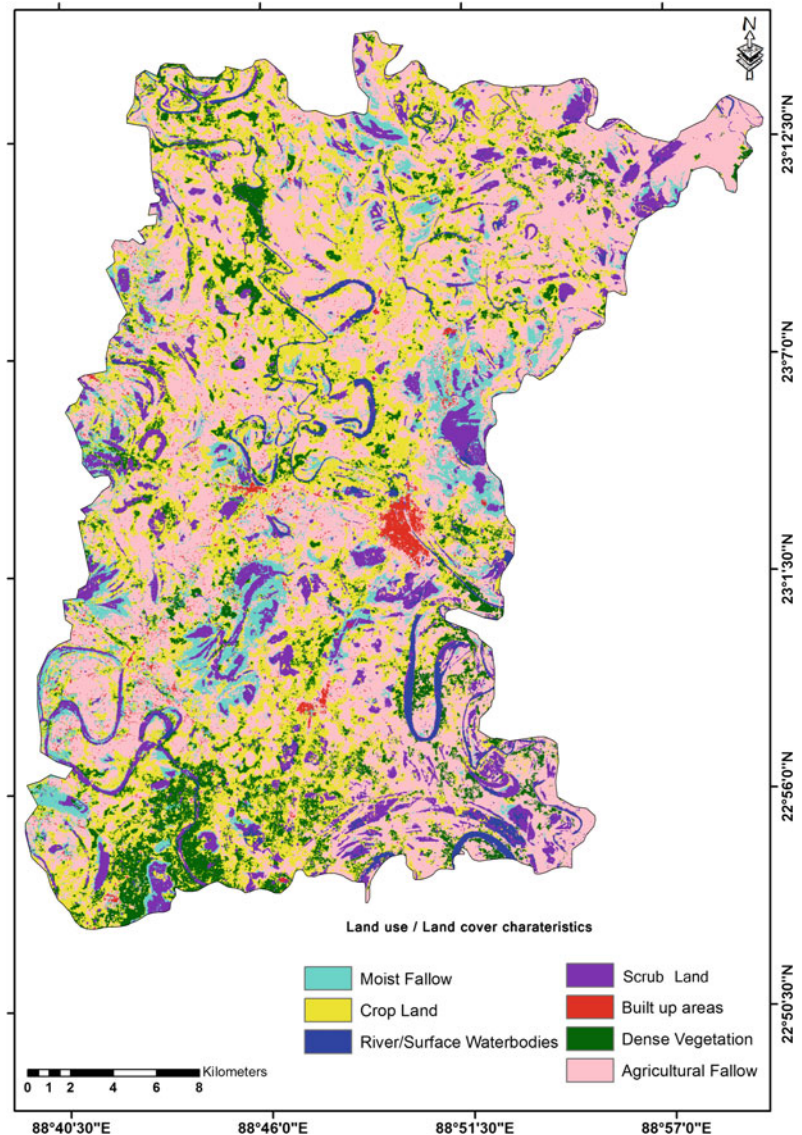
to flood hazards in the Bongaon sub-division. The rating has been decreased with the increasing distance from the river channel due to a decrease in ferocity (Fig. 4.11).

The road densities played a significant role in flood hazards as it is disturbing the free flow of water and restrict the passage of flood discharge. The road density of the Bongaon sub-division has been categorized into 5 sub-zones (Fig. 4.12). The higher road density was assigned a low rating and the lower road density region was demarcated as a higher rating for flood hazard. Following the very high susceptibility to flooding class, there was a class very high (<0.59 per km^2), 0.60 – 0.76 per km^2 graded

as class 2, 0.77 – 0.92 per km^2 placed as class 3, 0.93 – 1.1 per km^2 ranked as class 4 and very low ranked as >1.2 per km^2 .

The calculated flood risk index values of the output database vary from 0.05 (Low) to 0.68 (High) (Table 4.3). The derived flood risk map was reclassified into five categories through manual classification methods in ArcGIS software, such as: (i) very low risk (less than 0.15), low risk (0.16–0.26), medium risk (0.27–0.33), high risk (0.34–0.48), and very high risk (more than 0.49) (Fig. 4.13). The ‘medium risk’ is measured along the areas that might be seasonally overwhelmed in the wet season. The ‘very low risk’ refers to the areas prone to very low

Fig. 4.6 Reclassified land use/land cover map of Bongaon sub-division

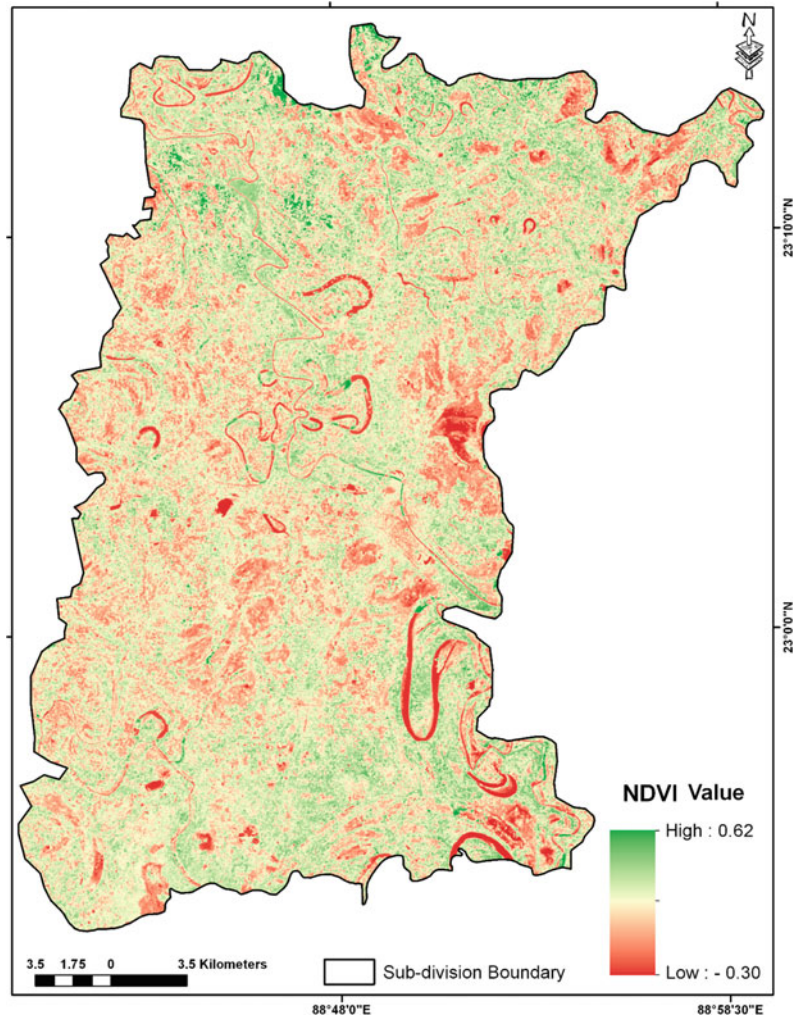


occurrences of floods, almost nil. Moreover, the ‘very high risk’ and ‘high risk’ zones of flood denote the conceivable areas of flood that can eventuate because of the periodic as well as intermittent heavy rainfall.

Zonal statistical tool of ArcGIS software v9.3 was used to determine the areal distribution of flood risk areas of the Bongaon sub-division. The flood risk map portrays that probably 74.70 km² (8.96%) of the area comes under very high flood risk areas (Table 4.3). These areas were mostly distributed in the south-east, north, north-east

and some small pockets of the central part of the Bongaon sub-division. Approximately, 19.36% (161.45 km²) of the area falls under high risk, distributed in the eastern and northern part of the sub-division. The medium flood risk areas are calculated as 242.02 km² (29.02%), distributed in the central north, north-west and south-west part of the study site. About 28.33% (236.33 km²) of the Bongaon sub-division falls under the low flood risk areas which are disseminated in the central, southern and western part of the sub-division (Fig. 4.13).

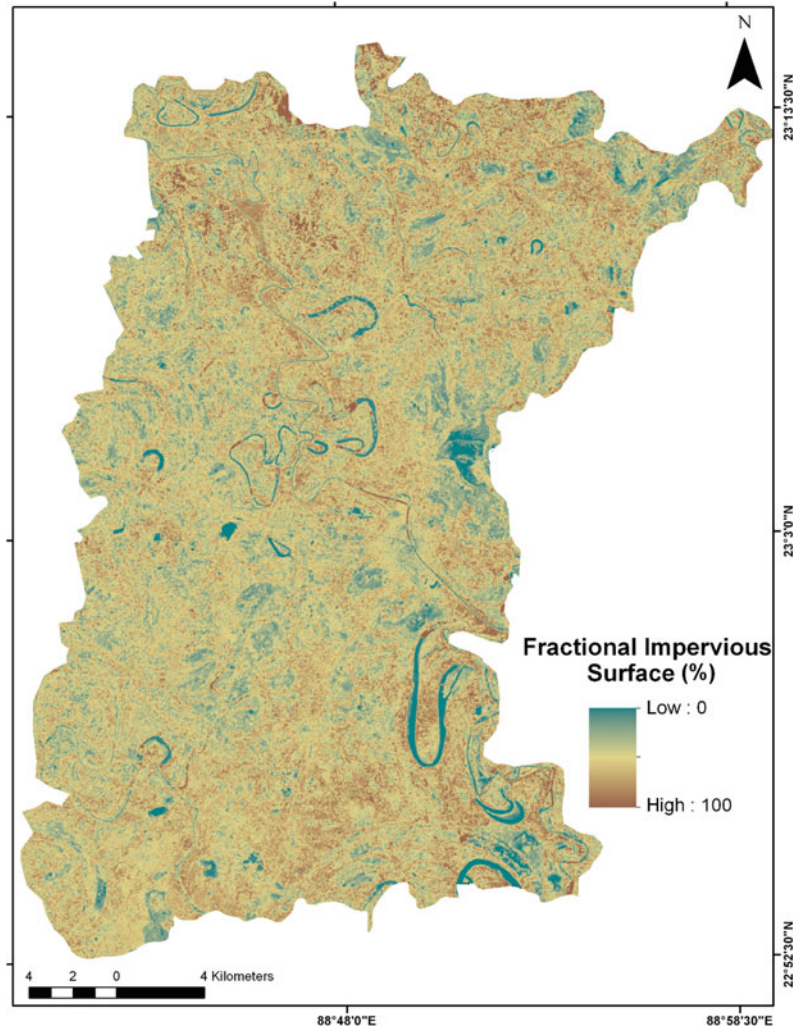
Fig. 4.7 Reclassified vegetation characteristics (NDVI) map of Bongaon sub-division



A total of 55 sites were designated to measure the flood substantiations events (Table 4.4). These points are distributed in different directions of the sub-division and distributed in the entire region of the sub-division. Chronological floods events were used as verifications sites. There were 13 sites (VP1, VP2, VP4, VP12, VP17, VP18, VP19, VP20, VP37, VP43, VP44, VP45 and VP46) of ‘very high’ risk of flood events and eight sights (VP6, VP14, VP25, VP30, VP31, VP42, VP5 and VP55) of ‘high’ risk for flood events were checked. The medium flood risk validation points are demarcated as VP10, VP13, VP16, VP23, VP27, VP29, VP36 and VP52. These areas are usually waterlogged

for 3 to 4 days or a short duration of the flood because of the concentrated rainfall events. The low flood risk validation points are designated as VP3, VP7, VP8, VP21, VP26, VP32, VP39, VP40, VP49 and VP51. The user accuracy and producer accuracy of low flood risk areas were calculated as 89% and 80%, respectively. Moreover, VP5, VP9, VP11, VP15, VP22, VP28, VP33, VP34, VP35, VP38, VP41, VP47, VP48, VP50 and VP53 are considered as very low risk. These areas were not also inundated since 2005 and mostly characterized by high elevation, far from the river channel, dense vegetation cover, protected from the flood by anthropogenic activities. The user’s accuracy and

Fig. 4.8 Reclassified Fractional Impervious Surface (FIS) map of Bongaon sub-division



producer's accuracy of the predictive map of flood hazard in the Bongaon sub-division were calculated as 69% and 72%, respectively. Hence, the result of the analysis indicated that the methodology is satisfactorily consistent for substitute response.

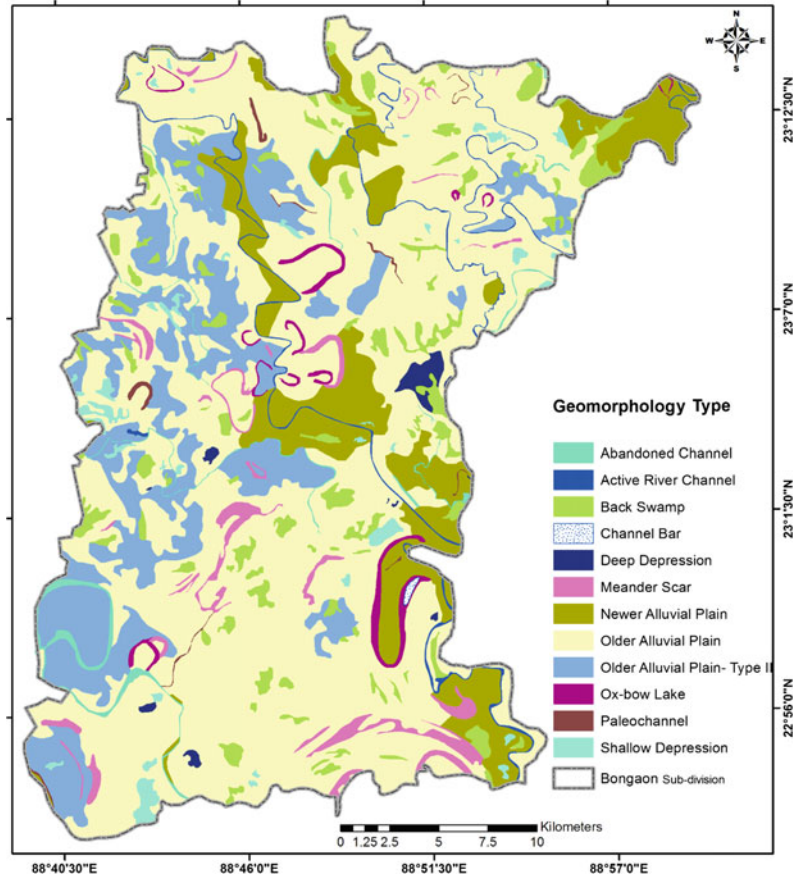
4.5 Discussion

Due to geographical characteristics, unplanned infrastructure and land use planning have a high level of flood risk. Flooding has become a regular phenomenon and continues to threaten the vulnerable social and economic infrastructure of the

sub-division. A flood risk map is a vivacious constituent for apposite land use forecasting in flood susceptible spaces. It produces easily read, quickly reachable graphs and diagrams which assists the superintendents and architects to categorize the extents of threat and highlight their vindication exertions (Gitikaand Ranjan 2016). Moreover, the flood vulnerability maps are intended to proliferate cognizance of the possibility of the drowning among the civic, indigenious specialists and other establishments by endorsing greater sentience of the risk of flooding.

The spatial variability of slope in the Bongaon sub-division is less, however, it plays an

Fig. 4.9 Reclassified geomorphological map of Bongaon sub-division

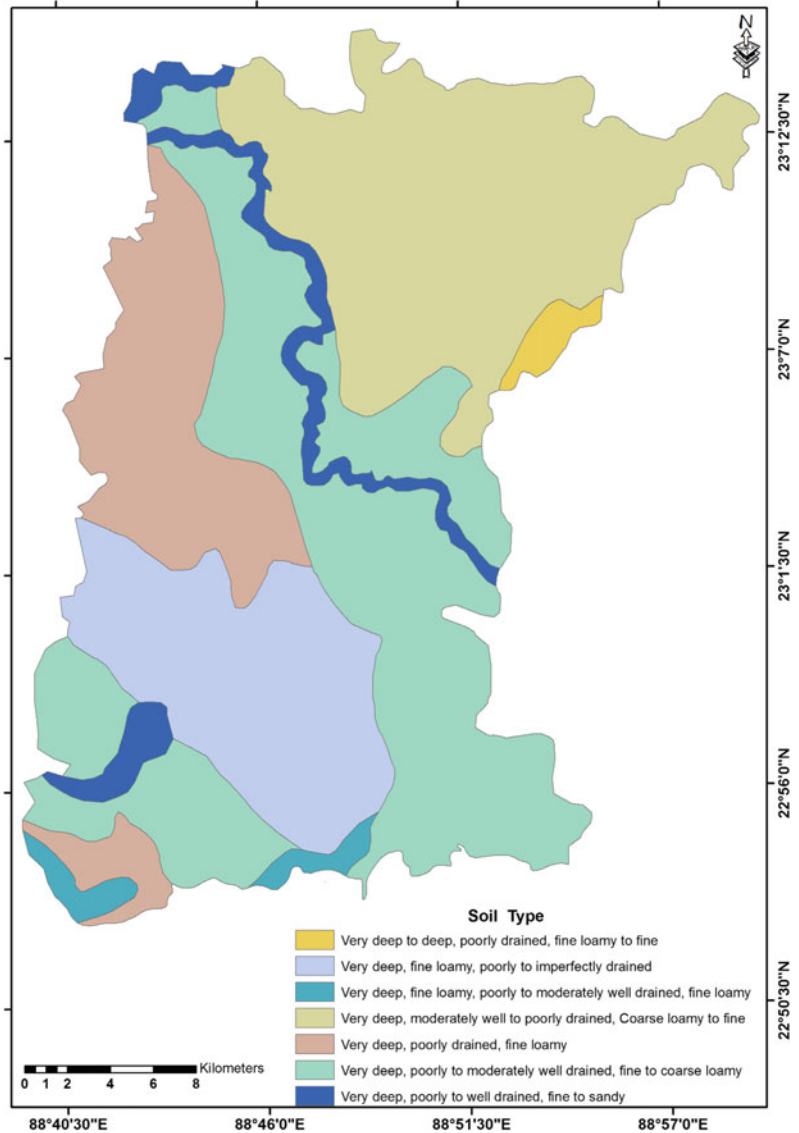


important role in hydrodynamic friction for flash flood simulation. The amount of water infiltration is reliant upon the peripheral aspects and soil properties, which differ based on the form of soil (Tejedor et al. 2013), types and texture (Nyarko 2002). Loamy soil water permeation is a factor that prerequisites to explain the processes of runoff, soil loss and aquifer recharge in addition to irrigation management and plant water convenience (Rimba et al. 2017). Population density is higher in lower elevated and flat areas and these areas have a very high liability to flash flooding. Additionally, descending areas should also be a focus as these are predisposed to descend during flood events (Cao et al. 2016). So,

the increase of sedimentation in river water caused loss of navigation which is also a great threat to the ecological balance of the river basin (Adel 2012).

The relationship between the occurrence of flooding and the classes of each conditioning factors was analysed. The elevation analysis outcomes designate that the lowest elevation was most persuasive on flooding. Moreover, results also showed that lower slopes along the eastern and northern parts of the sub-division inferred greater occurrence of flooding. Due to the lower slope, the speed of water flow has been lessened and upsurges the time for absorption and infiltration of water into the ground (Alemayehu

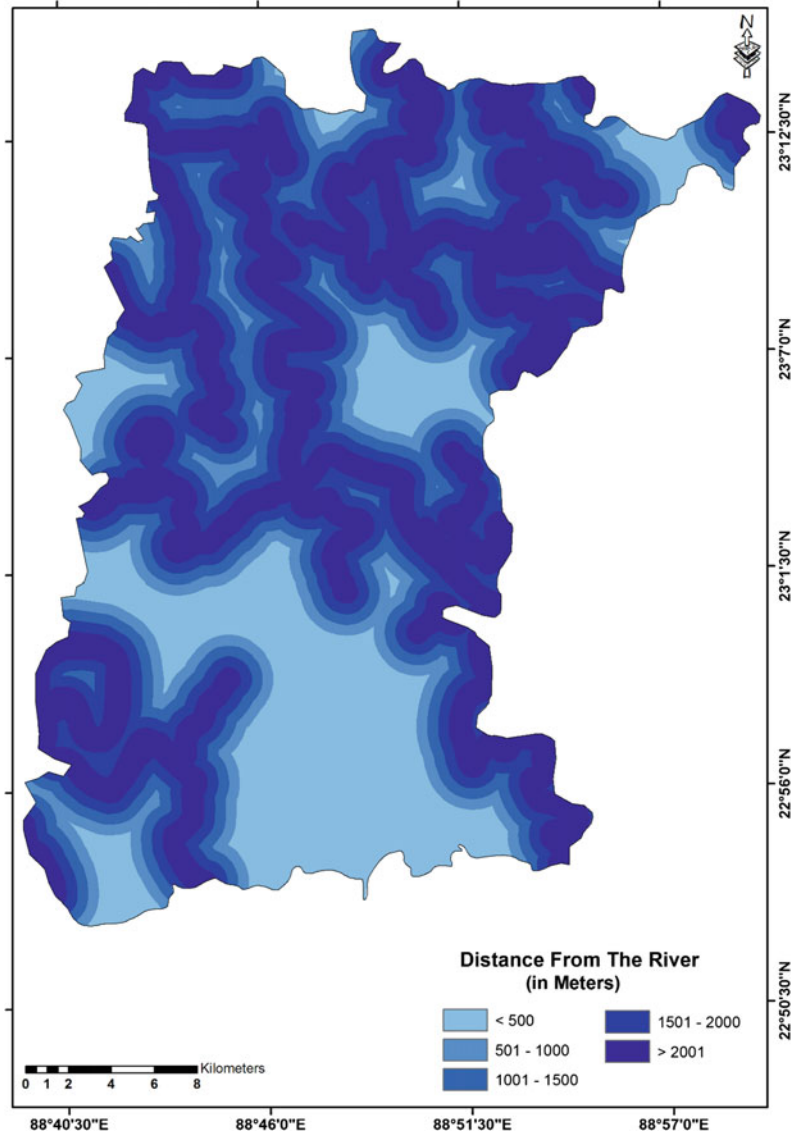
Fig. 4.10 Reclassified soil map of Bongaon sub-division



2007). The slope encourages the direction of the amount of surface runoff (Dai et al. 2002), and have a leading effect on the impact of rainfall to streamflow (Sawyer et al. 2004). According to Krumbein (1965), a flat surface is disposed to waterlogging; whereas, the steeper slope allows water to flow speedily. In the Bongaon sub-division, a high grade is consigned to less than 1° slope for the gentle gradient of the flood plain;

whereas, a little score is apportioned for the slope of more than 4.1° . Due to the heavier rainfall during flooding, river levels will increase and causing an overflow of water into areas closest to the riverbank. Road density is also a major factor of flood susceptibility mapping as it decreased the infiltration capacity of the terrain and is a source of runoff (Tehrany et al. 2017). The physical properties of the soil were considered to

Fig. 4.11 Reclassified distance from the river map of Bongaon sub-division



develop soil type factors. In the Bongaon sub-division, sandy soil has greater hydraulic conductivities than better-textured soils because of the great pore space between the soil elements. An earlier study also reported that the infiltration rate of the sandy soils is much higher than the clayey soil (Wondim 2016). Moreover, the areas situated adjacent to the main river channel and flow accumulation path are prone to

flood (Islam and Sado 2000). Mojaddadi et al. (2017) suggested that soil types have a straight influence on water stowage, penetrability and drainage.

LULC plays an important role in recognizing the sensitive regions prone to flooding. Areas covered with the vegetation compromise the levels of protecting appliances, creating land less lying to flooding and a negative relationship

Fig. 4.12 Reclassified road density map of Bongaon sub-division

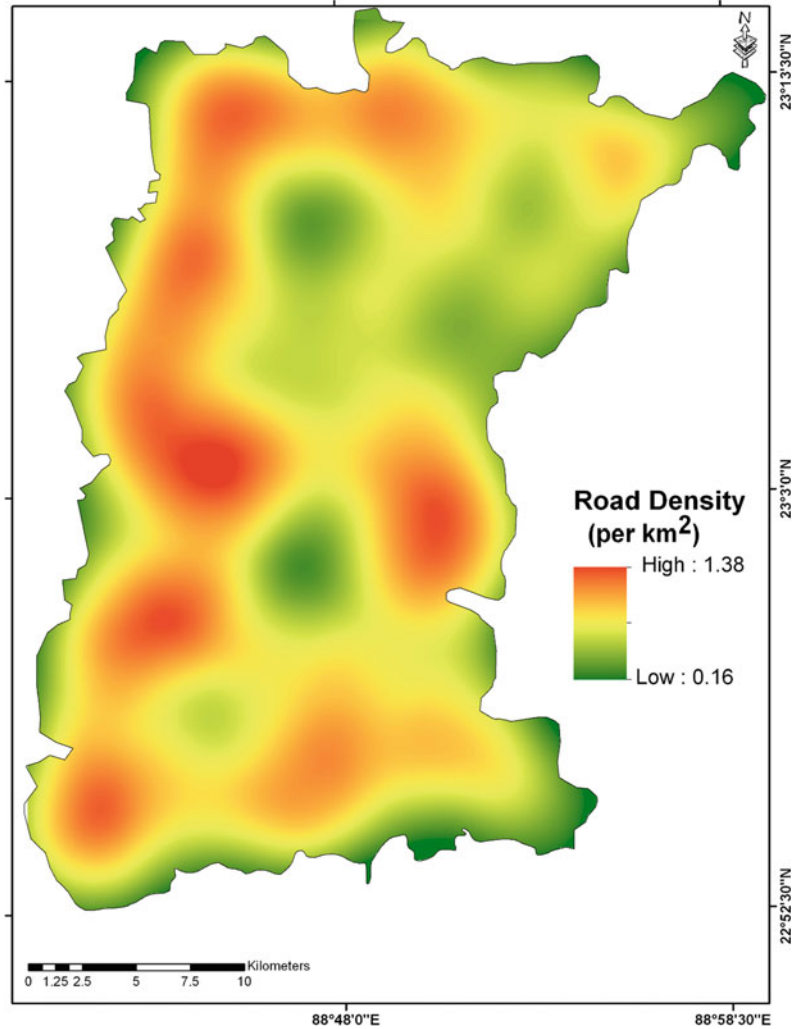


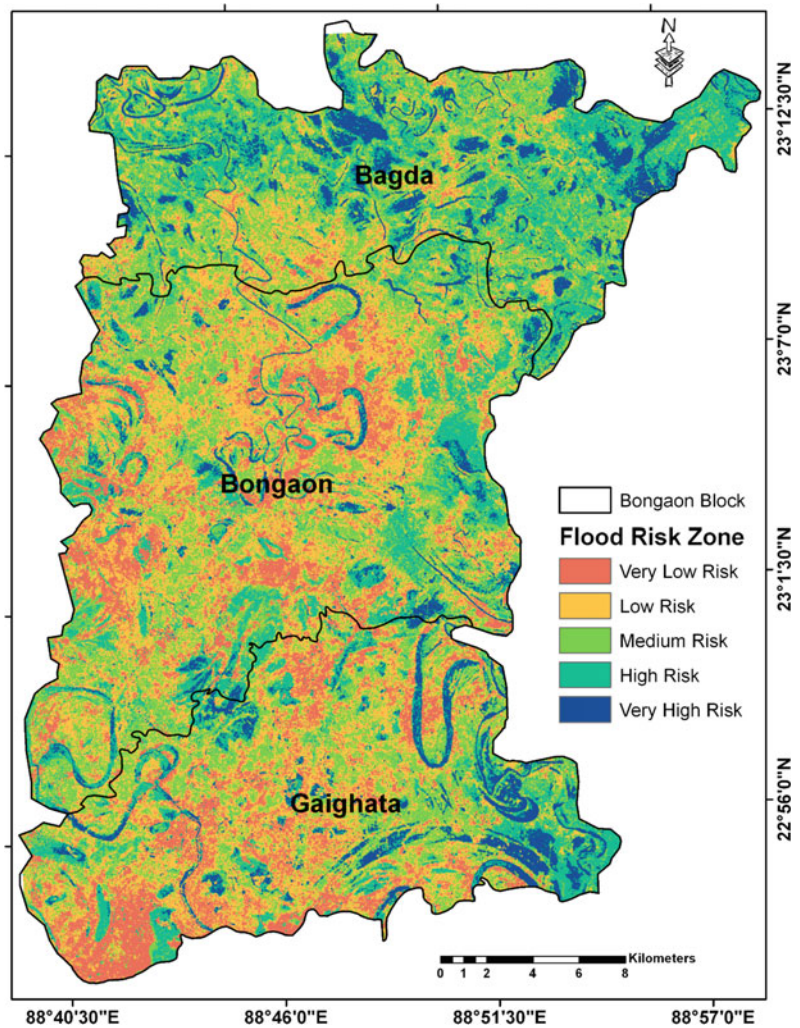
Table 4.3 Areal distribution of flood risk index map of the Bongaon sub-division

Flood risk index	Area (km ²)	Percent
Very low	119.55	14.33
Low	236.33	28.33
Medium	242.04	29.02
High	161.45	19.36
Very high	74.70	8.96

exists between a flood event and vegetation density (Al-Zahrani et al. 2016). LULC characteristics are a significant environment scheming the hazards as its solidities designate the appearance of the landscape and its geotechnical

chattels (Pareta 2004). The infringement of the areas are responsible for floods by human settlements and infrastructural development (Njoku et al. 2017). Results derived in this study also indicated that all NDVI classes of more than 0.24

Fig. 4.13 Flood risk map of Bongaon sub-division



have minimal impact on flood occurrence. The spatial extent of regional geomorphic features like new and old alluvial plain, meander scar, paleochannel, ox-bow lake, active river channel, abandoned river channel, natural depression, etc., are largely helpful in delineating flood susceptibility zone (Majumder et al. 2017).

However, the population density is very high in the sub-division due to its fertile alluvial plain (Paul and Chatterjee 2012; Jana et al. 2011). A huge chunk of settlements is observed in the sub-division and make some barriers (Saha 2015). Residents are using the riverbed as agricultural land for many decades. So, the increase of sedimentation in river water caused loss of

navigation, which is also a great threat to the ecological balance of the river basin (Adel 2012). Consequently, by the construction of a railway bridge at Majdia (Nadia District, West Bengal), a water barrier has been developed. The road is an important anthropogenic factor inducing flood hazards. Versini et al. (2010) stated that road network and traffic monitoring are a major cause for flood event managers. Consequently, by the construction of a railway bridge at Majdia (Nadia District, West Bengal), a water barrier has been developed. Valdiya (2004) reported that the obstructions caused by the construction of artificial infrastructures, considerably encumber the free flow of water.

Table 4.4 Assessment of the validation point of flood risk map of Bongaon Sub-division

Validation point (VP)	Ground observation/existing data base (2005–2016)	Flood risk index	Validation point (VP)	Ground observation/existing data base (2005–2016)	Flood risk index
VP1	2006–2009, 2011, 2013–2016	Very high	VP29	2007, 2008	Medium
VP2	2006–2009, 2011, 2013, 2015, 2016	Very high	VP30	2006–2009, 2015, 2016	High
VP3	Nil	Low	VP31	2007, 2011, 2015, 2016	High
VP4	2007, 2008, 2015, 2016	Very high	VP32	2007, 2008	Low
VP5	Nil	Very low	VP33	Nil	Very low
VP6	2007, 2008, 2015, 2016	High	VP34	Nil	Very low
VP7	2015	Low	VP35	Nil	Very low
VP8	2007, 2008	Low	VP36	2011, 2015, 2016	Medium
VP9	Nil	Very low	VP37	2006–2009, 2011, 2013–2016	Very high
VP10	2007, 2008	Medium	VP38	Nil	Very low
VP11	Nil	Very low	VP39	Nil	Low
VP12	2006–2009, 2015, 2016	Very high	VP40	Nil	Low
VP13	2006–2009, 2011, 2013, 2015, 2016	Medium	VP41	Nil	Very low
VP14	2007, 2008, 2015, 2016	High	VP42	2006 -2009, 2015, 2016	High
VP15	Nil	Very low	VP43	2006–2009, 2011, 2013–2016	Very high
VP16	2007, 2008, 2015	Medium	VP44	2006–2009, 2011, 2013–2016	Very high
VP17	2006–2009, 2011, 2013–2016	Very high	VP45	2006 -2009, 2015, 2016	Very high
VP18	2006–2009, 2011, 2013–2016	Very high	VP46	2007, 2008, 2015, 2016	Very high
VP19	2006–2009, 2011, 2013–2016	Very high	VP47	Nil	Very low
VP20	2006–2009, 2011, 2013–2016	Very high	VP48	Nil	Very low
VP21	2006–2009, 2011, 2013, 2015, 2016	Low	VP49	2007, 2008	Low
VP22	Nil	Very low	VP50	Nil	Very low
VP23	2007, 2008, 2015, 2016	Medium	VP51	2007, 2008	Low
VP24	Nil	Very low	VP52	2011, 2015, 2016	Medium
VP25	2007, 2008, 2015, 2016	High	VP53	Nil	Very low
VP26	2015	Low	VP54	2006 -2009, 2015, 2016	High
VP27	2007, 2008	Medium	VP55	2007, 2008, 2015, 2016	High
VP28	Nil	Very low			

4.6 Conclusion

The flood risk map of the Bongaon sub-division was generated through MCDA based on the integration of remotely sensed products and secondary datasets. The substantiation report advocates that remote sensing and GIS techniques are very influential approaches in flood risk exploration and planning. Eleven flood acclimatizing features were nominated and a flood inventory map was exploited to generate the flood dichotomous reliant layer. The MCDA method exposed in this research can be enriched further by counting these constraints, likewise rainfall, elevation, slope, distance from the river, road density, land use/land cover, etc. Hence, the extenuation actions can be accurately completed, and the controlling of flood menace is made easy. The generated flood risk map may be beneficial to proposers and creators for selecting an appropriate place for the forthcoming expansions and land use forecasting, and also to trace assemblies in the rickety regions. It could be of practice for specialists of the area for confirming security to the people of pretentious areas. This research also ropes the accompanying of the outmoded hydrological, with the contemporary geospatial tools, hence augmenting the assemblage, storage, analysis, management and demonstrating of flood data, along with being more cost, period and manpower competent.

References

- Adel MM (2012) Downstream ecocide from upstream water piracy. *Am J Environ Sci* 8(5):528–548
- Ajin RS, Krishnamurthy RR, Jayaprakash M, Vinod PG (2013) Floodhazard assessment of Vamanapuram River Basin, Kerala, India: An approach using Remote Sensing and GIS techniques. *Adv Appl Sci Res* 4(3):263–274
- Alemayehu Z (2007) Modeling of flood hazard management for forecasting and emergency response of 'Koka'rea within Awash River basin using remote sensing and GIS method. Unpublished Msc Thesis, AddisAbaba University, Ethiopia
- Alexakis DD, Grillakis MG, Koutroulis AG, Agapiou A, Themistocleous K, Tsani IK, Michaelides S, Pashiardis S, Demetriou C, Aristeidou K, Retalis A, Tymvios F, Hadjimitsis DG (2014) GIS and remote sensing techniques for the assessment of land use changes impact on flood hydrology: the case study of Yialias Basin in Cyprus. *Nat Hazards Earth Syst Sci* 14:413–426
- Al-Zahrani M, Al-Areeq A, Sharif HO (2016) Estimating urban flooding potential near the outlet of an arid catchment in Saudi Arabia. *Geomat Nat Hazards Risk* 1:1–17
- Basarudin Z, Adnan NA (2014) Impervious surface detection and mapping via digital remotely sensed techniques. In: *International Conference on Civil, Biological and Environmental Engineering (CBEE-2014)*, pp 27–28
- Cao C, Xu P, Wang Y, Chen J, Zheng L, Niu C (2016) Flash flood hazard susceptibility mapping using frequency ratio and statistical index methods in coalmine subsidence areas. *Sustainability* 8: 948. <https://doi.org/10.3390/su8090948>
- Chaturvedi R, Mishra SD (2015) Geomorphic features and flood susceptibility zones: A study for Allahabad district, Uttar Pradesh, India, using Remote Sensing and GIS technique. *Trans Inst Indian Geographers* 37(2):259–268
- Dai FC, Lee CF, Ngai YY (2002) Landslide risk assessment and management. An overview. *Eng Geol* 64:65–87
- Dandapat K, Panda GK (2018) A geographic information system-based approach of flood hazards modelling, Paschim Medinipur district, West Bengal, India. *Jamba (potchefstroom, South Africa)* 10(1):518. <https://doi.org/10.4102/jamba.v10i1.518>
- Dhruvesh KM, Praful MU, Aditya MV (2016) Flood hazard vulnerability mapping using remote sensing and GIS: a case study of Surat. *Res Rev: J Pure Appl Phys* 4(3):38–42
- Elsafi SH (2014) Artificial neural networks (ANNs) for flood forecasting at Dongola Station in the River Nile. Sudan. *Alexandria Eng J* 53(3):655–662
- Fustos I, Abarca-del-Rio R, Ávila A, Orrego R (2017) A simple logistic model to understand the occurrence of flood events into the Biobío River Basin in central Chile. *J Flood Risk Manag* 10(1):17–29
- Getahun YS, Gebre SL (2015) Flood hazard assessment and mapping of flood inundation area of the Awash river basin in Ethiopia using GIS and HEC-GeoRAS/HEC-RAS Model. *J Civil Environ Eng* 5:179. <https://doi.org/10.4172/2165-784X.1000179>
- Ghosh S, Mistri B (2015) Geographic concerns on flood climate and flood hydrology in monsoon-dominated Damodar river basin, Eastern India. *Geogr J Article ID* 486740, 16. <https://doi.org/10.1155/2015/486740>
- Gitika T, Ranjan S (2016) GIS-based flood hazard mapping: a case study in Krishnai river basin, India. *Res J Recent Sci* 5(ISC-2015):50–59
- Guhathakurta P, Menon PA (2011) Impact of climate change on extreme rainfall events and flood risk in India. *J Earth Syst Sci* 120(3):359–373
- Haq M, Akhtar M, Muhammad S, Paras S, Rahmatullah J (2012) Techniques of remote sensing and GIS for flood

- monitoring and damage assessment: a case study of Sindh province, Pakistan. *Egypt. J Remote Sens Space Sci* 15:135–141
- Islam M, Sado K (2000) Flood hazard map and land development priority map developed using AVHRR data with geographical information system. *Hydrol Process* 14:605–620
- Ismail M, Saanyol IO (2013) Application of remote sensing (RS) and geographic information systems (GIS) in flood vulnerability mapping: case study of River Kaduna. *Int J Geomat Geosci* 3(3):618–627
- Jana A, Ghorai D, Bhunia GS, Pal DK (2011) Demographic pressure in transforming of land use/ land cover over four decades in Nadia District of West Bengal province India using multi-temporal Landsat data. *Niugini Agrisaiens* 3:59–74
- Kazakis N, Kougiaris I, Patsialis T (2015) Assessment of flood hazard areas at a regional scale using an index-based approach and analytical hierarchy process: application in Rhodope-Evros region, Greece. *Sci Total Environ* 538:555–563
- Krumbein WC, Graybill FA (1965) *An introduction to statistical models in Geology*. Mc Graw Hill, New York, p 475
- Lim J, Lee K (2018) Flood mapping using multi-source remotely sensed data and logistic regression in the heterogeneous mountainous regions in North Korea. *Remote Sens* 10(7):1036
- Majumder R, Ghosh DK, Mandal AC, Patra P, Bhunia GS (2017) An appraisal of geomorphic characteristics and flood susceptibility zone using remote sensing and GIS: a case study in Bongaon Subdivision, North 24 Parganas (West Bengal). *India. Int J Res Geogr (IJRG)* 3(4):32–40
- Mandal S, Mandal B (2015) Assessment and prediction of slope instability in the Lish River Basin of Eastern Darjiling Himalaya using RS and GIS. *Int Res J Earth Sci* 3(12):9–20
- Matori AN, Lawal DU, Yusof KW, Hashim MA, Balogun A (2014) Spatial analytic hierarchy process model for flood forecasting: an integrated approach. In: 7th IGRSM international remote sensing and GIS conference and exhibition, IOP conference series: earth and environmental science, vol 20, p 012029
- Mukherjee A (2006) Deeper groundwater flow and chemistry in the arsenic affected Western Bengal Basin, West Bengal, India. University of Kentucky Doctoral Dissertations, Paper 368. http://uknowledge.uky.edu/gradschool_diss/36
- Nandargi S, Dhar ON (2003) High frequency floods and their magnitudes in the Indian rivers. *J Geol Soc India* 61(1):90–96
- Nugraha AL, Awaluddin M, Sasmito B (2018) Modelling multi hazard mapping in Semarang city using GIS-fuzzy method. In: 2nd geoplanning-international conference on geomatics and planning. IOP conference series: earth and environmental science, vol 123, p 012002. <https://doi.org/10.1088/1755-1315/123/1/012002>
- Ouma YO, Tateishi R (2014) Urban flood vulnerability and risk mapping using integrated multi-parametric AHP and GIS: methodological overview and case study assessment. *Water* 6(6):1515–1545
- Pareta K (2004) Hydro-geomorphology of Sagar District (M.P.): a study through remote sensing technique. In: *Proceeding in XIX M. P. Young Scientist Congress*, Madhya Pradesh Council of Science & Technology (MAPCOST), Bhopal
- Patel DP, Srivastava PK (2013) Flood hazards mitigation analysis using remote sensing and GIS: correspondence with town planning scheme. *Water Resour Manag* 27:2353–2368
- Paul S, Chatterjee K (2012) Urbanisation and consistency measurement: a study on district of north 24 Parganas, West Bengal. *India. Arch Appl Sci Res* 4(5):2052–2067
- Pradhan B (2011) Use of GIS-based fuzzy logic relations and its cross application to produce landslide susceptibility maps in three test areas in Malaysia. *Environ Earth Sci* 63:329–349
- Rahmati O, Pourghasemi HR, Zeinivand H (2016) Flood susceptibility mapping using frequency ratio and weights-of-evidence models in the Golistan Province. *Iran. Geocarto Int* 31(1):42–70
- Rimba AB, Setiawati MD, Sambah AB, Miura F (2017) Physical flood vulnerability mapping applying geospatial techniques in Okazaki City, Aichi Prefecture, Japan. *Urban Sci* 1:7. <https://doi.org/10.3390/urbansci1010007>
- Roy SK, Sarker SC (2016) Integration of remote sensing data and GIS tools for accurate mapping of flooded area of Kurigram, Bangladesh. *J Geogr Inf Syst* 8:184–192
- Saha M (2015) Human interference in the resource utilization of Bongaon sub-division in north 24 Parganas district of West Bengal. *RJSSM* 5(8):120–129
- Samanta S KC, Pal DK, Palsamanta B (2016) Flood risk analysis in lower part of Markham river based on multi-criteria decision approach (MCDA). *Hydrology* 3(29):1–13. <https://doi.org/10.3390/hydrology3030029>
- Sawyer CF, David RB (2004) Landslide aspect: a methodological approach to circular data for hazard analysis. In: *Proceedings of the Applied Geography Conference*, 27, St. Louis, M.O, pp 67–74
- Sengupta S (1966) Geological and geophysical studies in western part of Bengal Basin, India. *Bull Am Assoc Petrol Geol* 150:1001–1017
- Stefanidis S, Stathis D (2013) Assessment of flood hazard based on natural and anthropogenic factors using analytic hierarchy process (AHP). *Nat Hazards* 68:569–585
- Tehrany MS, Pradhan B, Mansor S, Ahmad N (2015) Flood susceptibility assessment using GIS-based support vector machine model with different kernel types. *Catena* 125:91–101
- Tehrany MS, Shabani F, Jebur MN, Hong H, Chen W, Xie X (2017) GIS-based spatial prediction of flood

- prone areas using standalone frequency ratio, logistic regression, weight of evidence and their ensemble techniques. *Geomat Natl Hazards Risk* 8(2):1538–1561. <https://doi.org/10.1080/19475705.2017.1362038>
- Tejedor M, Neris J, Jiménez C (2013) Soil properties controlling infiltration in volcanic soils (Tenerife, Spain). *Soil Sci Soc Am J* 77:202–212
- Valdiya KS (2004) Lessening the ravages of floods. In: *Geology, Environment and society*. Universities Press, India, pp 112–115
- Versini PA, Gaume E, Andrieu H (2010) Assessment of the susceptibility of roads to flooding based on geographical information—test in a flash flood prone area (the Gard region, France). *Nat Hazards Earth Syst Sci* 10:793–803
- WMO (World Meteorological Organization) (2013) Integrated flood management tools series flood mapping. Issue 20, November 2013. https://library.wmo.int/pmb_ged/ifmts_20.pdf
- Wondim YK (2016) Flood hazard and risk assessment using GIS and remote sensing in lower Awash sub-basin, Ethiopia. *J Environ Earth Sci* 6(9):69–86